Variation of spatial and temporal characteristics of reactive flow in a periodically driven cavity: Gelation of sodium acrylate

M. Harini, S. Sriram, Abhijit P. Deshpande,* and S. Pushpavanam
Department of Chemical Engineering, Indian Institute of Technology Madras, Chennai 600036, India
(Received 14 May 2008; published 19 September 2008)

A reactive flow, the gelation of sodium acrylate (SA), was carried out in a cuboidal cavity with the top surface undergoing sinusoidal periodic motion. The instantaneous two-dimensional planar velocity fields during gelation were obtained using particle image velocimetry. The experiments were carried out with different plate velocities and different amounts of accelerator (TEMED). The temporal and spatial variations of the velocity components were analyzed. The magnitude of the velocity components was found to decrease with the progress of reaction due to gel formation. The role of mixing on the reaction is understood from the amount of gel formed at different plate velocities. Gel formation patterns are explained in terms of the mixing characteristics of the periodic flow. The periodic variation of point velocities showed the presence of higher harmonics in the flow.

DOI: 10.1103/PhysRevE.78.031407 PACS number(s): 82.70.−y, 47.70.Fw, 47.85.md, 83.60.Df

I. INTRODUCTION

Network-forming material systems or gels exhibit a rich variety of deformation and transport behavior, while the network formation (or gelation) processes are underway as well as in their networked state. Rheological properties during and after gelation are important in understanding the processing behavior and properties of these material systems. The evolution of relaxation times and other rheological characteristics has been studied for various gel-forming polymers [1]. In applications, mold-filling operations, which are used for processing, involve complex geometries [2,3]. Both simulation and experimental investigations focus on engineering operating parameters such as mold-filling time, flow rate, and reaction rate [3]. In recent times, flow and gelation have been exploited in microfluidic devices for material synthesis [4,5]. Therefore, detailed understanding of the flow of reacting network-forming polymers is very important.

Benchmark geometries such as tube, annulus, rotating parallel disk, and sudden expansion are widely used to study the flow behavior of Newtonian and viscoelastic fluids. Thomas *et al.* have studied the patterns formed by a viscoelastic, dilute polymer solution in a Taylor-Couette flow using dynamic simulations based on the first principles [6]. They observed varied spatiotemporal patterns, such as diwhirls, rotating standing waves, and oscillatory strips, depending on the ratio of fluid relaxation time to the time period of the inner cylinder rotation. Flow in cavities is a one such benchmark problem for various flow situations in the processing industry, particularly in injection molding and die casting [7]. The cavities investigated in the literature include steady lid-driven cavities with one or two moving boundaries and periodically lid-driven cavities [8–12]. There is a wealth of literature available in both computational and experimental studies on the lid-driven cavity flows of Newtonian fluid [12–14]. Cavity flows become more complex when the fluid is non-Newtonian. Leong and Ottino were the first to experimentally examine the effect of viscoelasticity in cavity flows and found that the extent of mixing was weaker in non-Newtonian flows than in Newtonian flows under similar time periodic boundary conditions [15]. They also found that for low Reynolds number the viscoelastic fluid behaved similarly to the Newtonian fluid. Pakdel *et al.* studied the dynamics of viscoelastic fluid flow in lid-driven cavities using laser Doppler velocimetry and digital particle image velocimetry for a range of Deborah numbers (De) and aspect ratios [16]. They found that at larger De, the fluid motion became unstable and three dimensional. Moreover, they found that elastic effects break the symmetry observed in the cavity flows of viscous Newtonian fluids at low Reynolds number. Three-dimensional spiral flow behavior was observed in the cavity and was related to the normal stress effects arising from elasticity of the viscoelastic fluid [17].

The knowledge of macroscopic flow behavior, bulk flow properties under shear, and extensional flows is essential for processing applications. The cross-linking reaction is one such example of a reactive flow which has complex flow behavior accompanied by a phase change (from liquid to solid). During cross-linking the material undergoes a very rapid change in its molecular structure and properties. Mixing and shaping operations in polymer processing require sufficient mobility, which vanishes when the motion slows down near the gel point [1]. In this work, the reactive flow during cross-linking of sodium acrylate gelation was investigated in a periodically driven cavity. Instantaneous planar flow fields were obtained as the gelation proceeded. The spatial and temporal variations were analyzed along with streamline patterns and spectral analysis at differents point in the cavity.

II. EXPERIMENTAL DETAILS

A. Materials

Acrylic acid (99%) stabilized with 200 ppm hydroquinone monoethylether, sodium hydroxide (98%),

*Author to whom correspondence should be addressed: abhijit@iitm.ac.in

N,N′-methylene(bisacrylamide) (BAAm) (99.5%), ammonium per sulphate (APS) (98.5%), and N,N,N′,N′-tetramethylethylenediamine (TEMED) (99%) (Sisco research laboratories, India) were used as received.

B. Sample preparation

The monomer, sodium acrylate (SA), solution was prepared by neutralizing diluted acrylic acid with stoichiometric amount of diluted sodium hydroxide. The cross-linker, BAAm of 0.04 g, was added per 10 ml of neutralised solution. The mixture was heated at 50 °C until BAAm gets dissolved completely and the solution was cooled to room temperature. Soon after the initiator, APS of 0.005 g per 10 ml of solution was added followed by the addition of five drops of accelerator, TEMED.

C. Polymerization of sodium acrylate

Poly sodium acrylate gel was prepared by chemical cross-linking processes induced by free radicals, called free-radical-initiated polymerization. The first step in the gel formation process is the reaction between APS and TEMED in which the TEMED molecule is left with an unpaired valence electron, which is the free radical. The activated TEMED molecule can combine with an SA (or BAAm) monomer, during which the unpaired electron is transferred to the SA unit, so that it in turn becomes reactive. Another monomer can therefore be attached and activated in the same way. The polymer can continue growing with the active center being continually shifted to the free end of the chain. Thus forming a solidlike gel.

D. Rheology

Linear rheology was investigated using "Anton Paar Rheometer, Physica (MCR-301)" on a cone and plate geometry (25 mm diameter, 0.047 mm gap, 1° cone angle). Oscillatory and steady-shear measurements were carried out at 20 °C during gelation.

E. Flow field measurement

Particle image velocimetry (PIV) (LaVision GmBH, Germany) was used to obtain accurate quantitative information of the instantaneous planar velocity field. The velocity fields in fluids are calculated by tracking the motion of the seeding particles (neutrally buoyant fluoroscent particles). Two images of the particle flow field are taken [charge-coupled-device (CCD) camera, 1024×1280] separated by a small amount of time (Δt). The distance traveled by the particles over Δt was determined by cross correlating the two images. With the distance and time known, velocity vectors were calculated. The measurements were carried out in the x-y plane (center of the cavity along the z direction). The geometric details and schematic of the experimental setup are shown in Fig. 1. Temporal variations of computed velocity fields (x component u, y component v) were extracted at characteristic points 1, 2, 3, 4, and 5 as shown in Fig. 2: point 1, which is close to the top corner of the wall, where the flow is equally dominant in both the directions; point 2 to the top center and point 5 at the center of the cavity, where flow is dominant in the x direction. Therefore v is very much smaller than u. Point 3 is at the top corner of the cavity and point 4 at the bottom of the cavity. When plate moves from extreme right towards center it is noted as position 1 and from center to extreme left as position 2. Positions 3 and 4 are mirror images of positions 1 and 2, respectively.

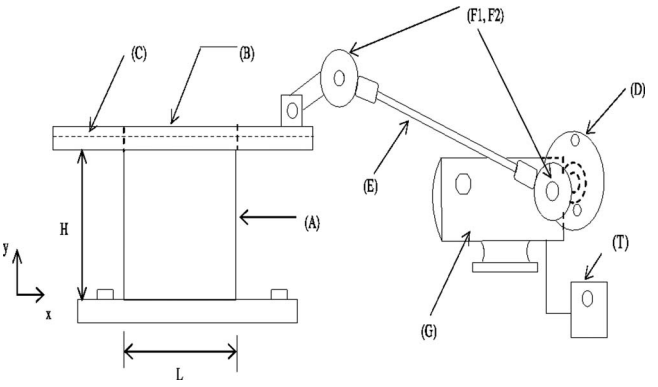

FIG. 1. Schematic diagram of the experimental setup. The letters indicate (A) cavity, (B) top plate, (C) guide plate arrangement, (D) drive wheel, (E) connecting rod assembly, (F1, F2) ball bearings, (G) permanent magnet dc motor, and (T) thyristor drive.

III. RESULTS AND DISCUSSION

A. Rheology during gelation

Rheological studies were performed during gelation by the oscillatory shear experiment, with a strain of 1%. The elastic moduli (G') and viscous moduli (G'') were monitored during the gelation (cross-linking) to study the viscoelastic response of the material. The time at which the loss factor ($\tan\delta = G''/G'$) becomes independent of frequency was inferred as the gel time in accordance with the Winter-Chambon criterion [18]. Figure 3(a) shows the plot of $\tan\delta$ as a function of time at different angular frequencies. The angular frequencies were varied from 1 to 100 s^{-1}. From the plot it can be observed that, as time progresses, the $\tan\delta$ values become identical (independent of frequency) at 250 s. Thus the gel time for the PSA system under study was found to be 250 s. The steady-shear experiment was performed to study the viscous response of the system during gelation. It

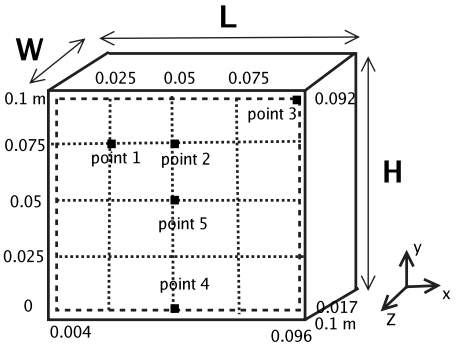

FIG. 2. Geometric details of the cavity.

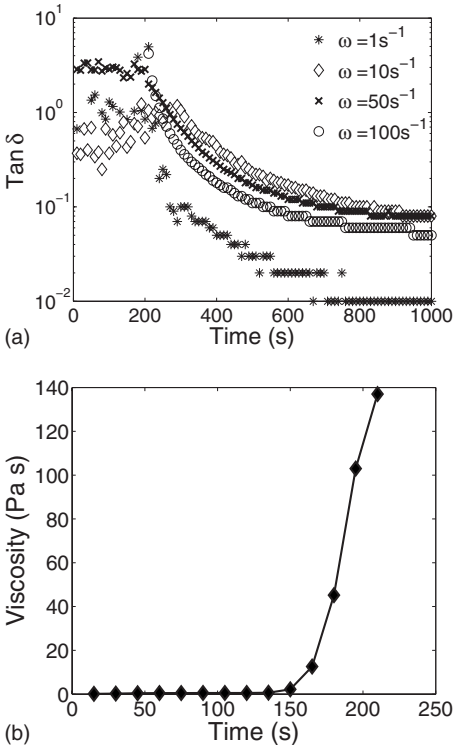

FIG. 3. (a) Variation of tan δ with time at different frequencies. Validity of the Winter-Chambon criterion (tan δ being independent of frequency) during gelation of PSA for the determination of gel time. (b) Gel time determination from the steady-shear experiment, at a constant shear rate of γ=1 s^{-1}.

yields an approximate estimate to determine gel time. Figure 3(b) shows the steady-shear response during the process; the time at which viscosity increases rapidly is termed the gel time. Here we see the increase in viscosity from 0.139 to 137 Pa at 210 s, which is close to the value obtained from the oscillatory shear measurements.

The oscillatory response during cross-linking at ω=1 s^{-1} with reaction time is shown in Fig. 4. From the figure it can be see that, initially G' was lower than G'', as the monomer solution is viscous (liquidlike) and there are not enough free radicals present to dominate the cross-linking. Later as the cross-linking dominates and elasticity sets in, there is an increase in G' at a much higher rate than G''. The reaction mixture at the gel point is referred to be in the *critical gel* state [1].

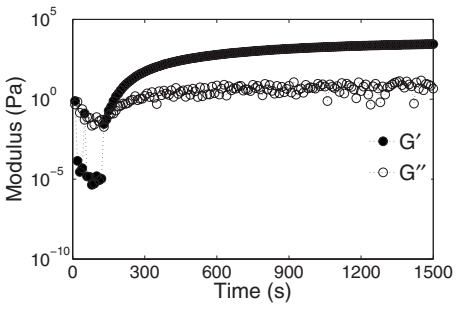

FIG. 4. Time sweep during cross-linking of PSA gel at constant frequency (ω=1 s^{-1}) showing the three regimes: viscous, viscoelastic, and viscoelastic solidlike.

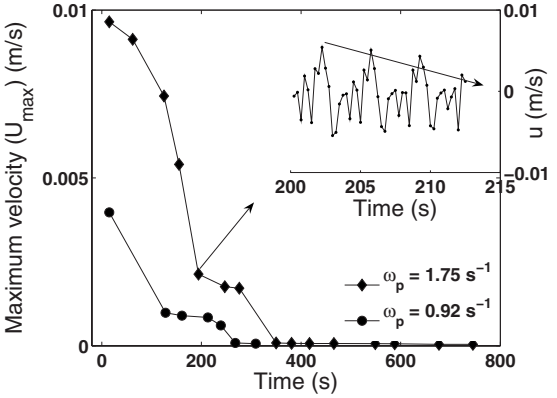

FIG. 5. Maximum velocity (U_{max}) at point 2 for different plate frequencies. The inset indicates the decrease in amplitude of the u component velocity for the set of data as pointed out by the arrow.

Based on these results, flow fields were characterized during gelation. At smaller times, predominantly viscous behavior of monomer solution (which is Newtonian in nature) was observed. Subsequently, as the gelation progresses, an increase in elasticity and viscosity was observed along with the liquid-solid transition. Finally, solidlike behavior of cured gel was observed.

B. Flow visualization during gelation

The time-dependent fluid flow in a square cavity was studied for gelation of PSA. For the PIV studies, SA monomer solution along with dissolved cross-linker, BAAm was taken in the cavity. Initially, periodic flow in the cavity was achieved with the mixed solution of two monomers (SA +BAAm). Once the system attained the periodic state, the initiator (APS) followed by accelerator (TEMED) were added through an injection port (provided at the center of the cavity). After immediate addition of accelerator the polymerization reaction starts. As the reaction proceeds, images were taken at different sets of time with certain time gaps until the velocity drops to zero. The drop in velocity is gradual as reaction mixture gains viscosity and elasticity, finally leading to gel formation. In the course of the process, the reactant mixture, which is Newtonian initially, becomes viscoelastic, with a sol-gel transition followed by a solidlike gel behavior at the end. Since lid motion is periodic, the velocities at all points in the cavity are also periodic. Unlike Newtonian and viscoelastic fluids, the amplitudes of velocity components change as a function of time due to progress in the reaction (as shown in the inset of Fig. 5).

The experiments were conducted at different plate velocities (ω_p=0.92 and 1.75 s^{-1}) and with different amounts of accelerator (0.2 and 0.4 ml).

1. Varying the speed of the top plate

The variation of amplitude of u at point 2 (as shown in Fig. 2) for different plate velocities is shown in Fig. 5. With an increase in the plate velocity, U_{max} increased. Additionally, the three regimes were identified clearly: initial phase of rapid decrease (until 200 s in Fig. 5 for ω_p=1.75 s^{-1}), a

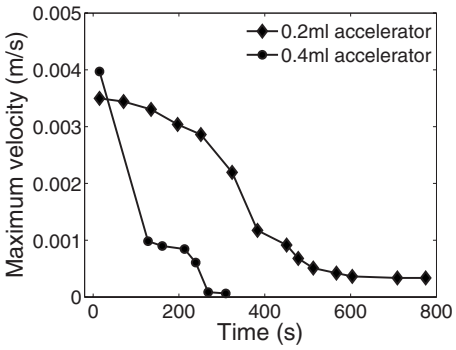

FIG. 6. Maximum velocity (U_{max}) at point 2 at plate frequency=0.92 s^{-1} for different amounts of accelerator.

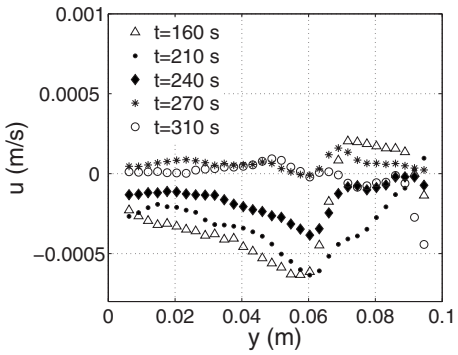

FIG. 7. Variation of u component velocity along x=0.05 m for 0.4 ml accelerator and ω_p=0.92 s^{-1}, at position 1 (when plate moves from extreme right towards the center of the cavity).

gradual decrease in U_{max} (from 200 to 380 s), followed by (very low) constant U_{max} with further increase in time. These three regimes can be made to correspond to the regimes observed (viscous, viscoelastic, viscoelastic solidlike) with rheological measurements as shown in Fig. 4. The initial drop in U_{max} was at 130 s. Also from the streamline patterns as discussed in the latter part of this paper, it can be said that the fluid behavior is Newtonian. This is reflected in oscillatory rheology as well, where G' is much smaller than G'' until 130 s (corresponding to viscous behavior of the fluid) as shown in Fig. 4. Later we see that $G' \sim G''$ around 200 s, which corresponds the viscoelastic behavior at 160 s. As time progresses (>200 s), we see that G' is always greater than G'', where the fluid is more solidlike and hence we see that the U_{max} is very small. The regime with a gradual decrease in velocity corresponds to the critical gel state. The time at which the velocity becomes close to zero is related to the gel time. In macroscopic flow, the gel formation would depend on local concentrations and therefore mixing. Therefore, the velocity data such as shown in Fig. 2 can be used to examine gel formation in different sections of the cavity.

2. Varying amount of accelerator

The amount of accelerator decides the time duration of gel formation during macroscopic flow. An increase in the amount of accelerator leads to an increase in the formation of the number of free radicals and lowers the reaction time. Hence the amount of accelerator is the rate-determining step here, unlike the rheological measurements where there is always an excess amount of accelerator (as very little sample is taken for rheological studies). Figure 6 shows the amplitude of u as a function of time at point 2. When a smaller amount of accelerator was used, it took longer to reach very low and constant values of the maximum velocity. The concentration of free radicals would be less, leading to a slower approach to local gelation. With a larger amount of accelerator (0.4 ml), gelation occurs around 250 s, which is closer to the rheological observations.

In order to observe the variations of flow structures with time, the spatial variation of velocities were analyzed across different planes. The spatial variation of u and v at plate position 1 along different planes is shown in Figs. 7 and 8, respectively. The variation of u along x=0.05 m at different time intervals is shown in Fig. 7. The profiles are depicted for position 1, when the plate moves from the extreme right towards the center of the cavity. Similarly the variation of v along y=0.075 m at different time intervals is shown in Fig. 8. A decrease in magnitude of u and v was observed with progress in the reaction. Contrary to Newtonian, viscoelastic, and power-law fluid behaviors, it is interesting to note that the magnitude of velocity was observed to be negative at 160 s. This indicates that the fluid is moving in the direction opposite to the motion of the plate. These observations were corroborated with streamline patterns as well in the later discussion of this article.

The streamline patterns were characterized with time at different plate positions for all the sets of experiments. The streamline patterns for 0.4 ml accelerator and top plate frequency ω_p=0.92 s^{-1}, at different flow regimes for positions 1, 2, 3, and 4, are shown in Figs. 9–11 at 130, 160, and 240 s, respectively. The units of X and Y coordinate values are in nm. These patterns were obtained from the interpolated data to track the exact positions of the plate.

These occurrences of positions are taken corresponding to the variation of velocity at point 2 (as shown in Fig. 2) with time. Initially, as the fluid behaves as a Newtonian fluid, positions 1 and 3 and positions 2 and 4 were found to be mirror images of each other until 130 s. Though they are mirror images, the streamline patterns of position 1 are entirely different than the Newtonian fluids when compared

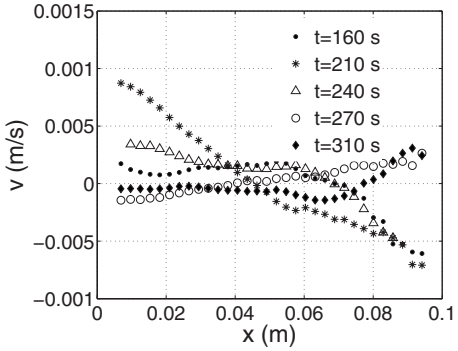

FIG. 8. Variation of the v-component velocity along y =0.075 m for 0.4 ml accelerator and ω_p=0.92 s^{-1}, at position 1 (when plate moves from extreme right towards the center of the cavity).

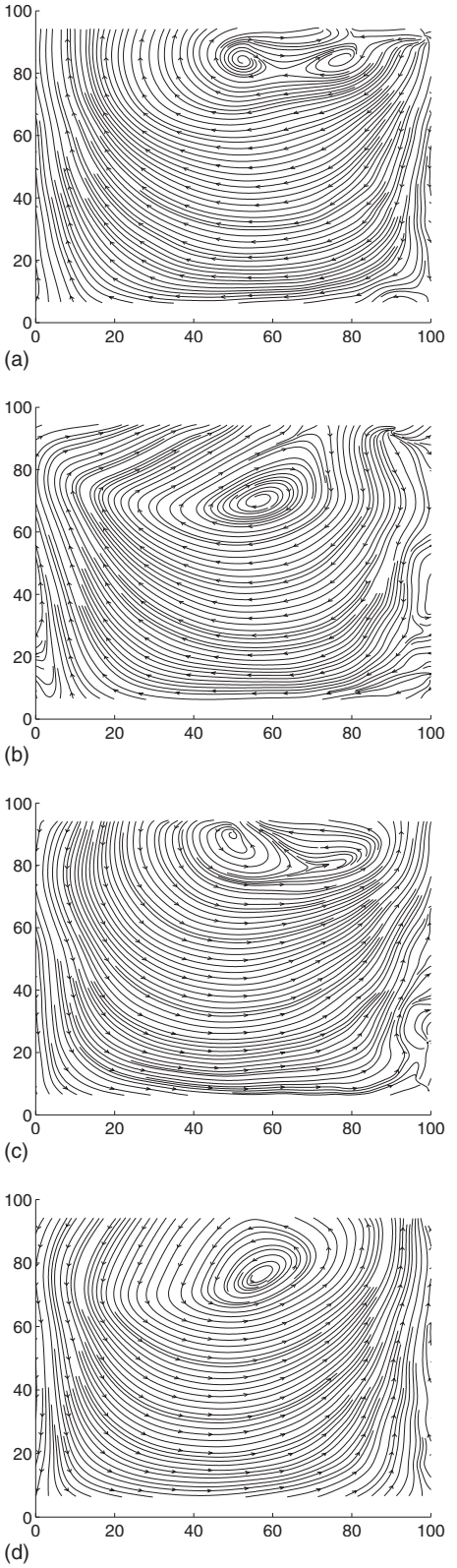

FIG. 9. Streamline patterns at (a) position 1, (b) position 2, (c) position 3, and (d) position 4 at $t=130$ s as the reaction proceeds.

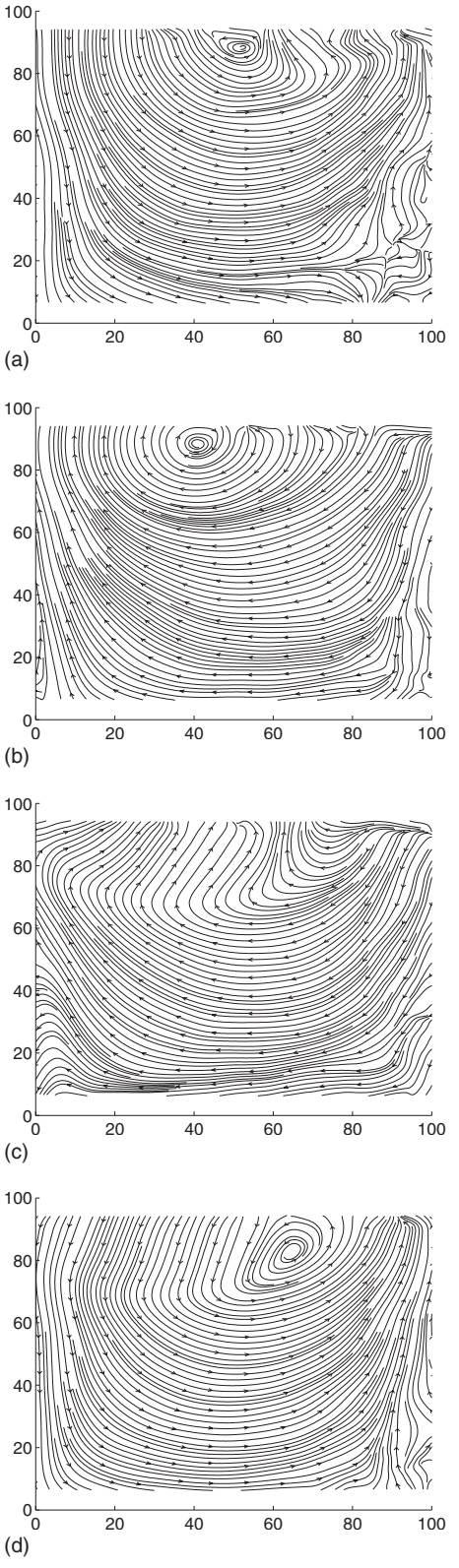

FIG. 10. Streamline patterns at (a) position 1, (b) position 2, (c) position 3, and (d) position 4 at $t=160$ s as the reaction proceeds.

with previous studies by Sriram *et al.* [12]. For Newtonian fluid in a periodically driven cavity, the streamline patterns at low Reynolds number show a primary vortex that fills up the entire cavity at all plate positions [12]. Since the viscous forces are dominant and these are bounded flows, we see circular streamline patterns, whereas in the reacting fluid the behavior is Newtonian until 130 s and thereafter it becomes a viscoelastic fluid. So at 130 s we see a single vortex filling

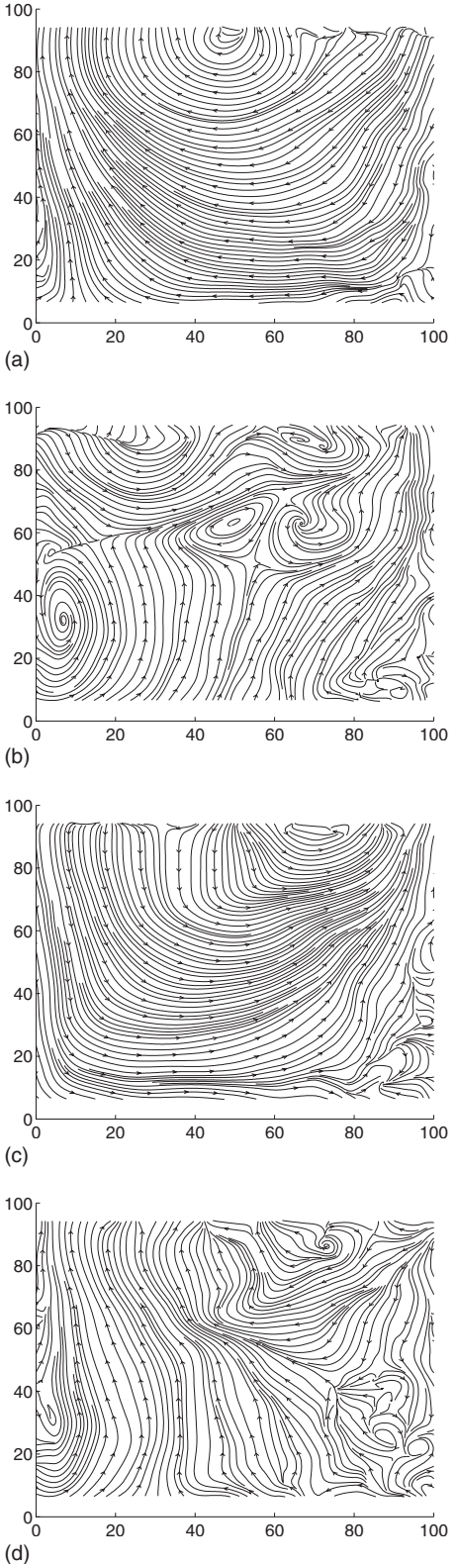

FIG. 11. Streamline patterns at (a) position 1, (b) position 2, (c) position 3, and (d) position 4 at $t=240$ s as the reaction proceeds.

the entire cavity at plate positions 2 and 4 only, while at positions 1 and 3 (where the plates are in extreme positions), the primary vortices are split.

With progression in time, we see the onset of viscoelasticity at 160 s, where the symmetry is lost (i.e., no mirror images were found). At 160 s we can see in Fig. 7 that the u velocity is negative. At all the earlier instants (data not shown), the velocity is positive. Therefore, the fluid velocity at this plate position reverses in direction as the gelation is approached (as shown in Fig. 10). The loss in symmetry for viscoelastic fluid flow has been observed by Pakdel *et al.* [16]. At 240 s, we observe complex patterns in streamlines, with multiple vortices filling the cavity in positions 2 and 4, as shown in Fig. 11. It should be noted that velocity is very low (as shown in Fig. 5) after the formation of gel (i.e., at times larger than 240 s). Overall, there is hardly any flow in the cavity at these times and, therefore, the complex patterns at these times arise due to decrease in the signal-to-noise ratio. The change in the streamline patterns with progress in the reaction is because of the change in fluid behavior and is also reflected in Fig. 5, where there is a sudden drop in the maximum velocity at point 2.

Upto 160 s, the changes in flow patterns are associated with gelation. Similar variations in velocity as well as streamline patterns were observed with different accelerator concentrations and plate speeds. In all the cases, the changes were observed near the critical gel (near the gel transition). At initial instants, flow patterns were largely similar to the case of Newtonian fluids. At very large time instants, flow in the cavity dies down. Therefore, material transformation or network formation processes affect the macroscopic flow near the critical gel state.

The detailed features of the pattern evolution can be highlighted, for example, the position of the vortex center at plate positions 2 and 4. As observed in Fig. 9, the vortex center is closer to the center at 130 s. At initial instants (data not shown), the vortex centers were observed to be very close to the moving plate. Therefore, the vortex center moves down with network formation and then moves up as critical gel is formed. The vortex center can be taken as an indication of the spatial extent of the momentum transfer by the moving plate. It is known that with increase in elasticity momentum transfer is over larger distances [19].

C. Power spectrum analysis

A power spectrum estimate of u and v was calculated at point 1, which is close to the wall (top left) of the cavity, point 2 at the top center of the cavity, point 3 at the top corner of the cavity, point 4 at the bottom of the cavity, and point 5, exactly at the center of the cavity, as shown in Fig. 2. The experimental data obtained from the PIV measurements were extracted at all these points, and a power spectrum estimate was calculated. Figure 12 shows the power spectra of u- and v-component velocities at point 2 for 0.4 ml addition of accelerator and $\omega_p=0.92$ s^{-1}. Multiple frequencies were appearing at points 1 and 2 for u and at points 2 and 5 for v. Initially at 15 s the fluid shows the same frequency as plate frequency as the fluid behaves like Newtonian. As for Newtonian fluid, it was shown by Sriram *et al.* [12] that u and v components have a single frequency as the plate frequency at point 1. At point 2, the u component shows the

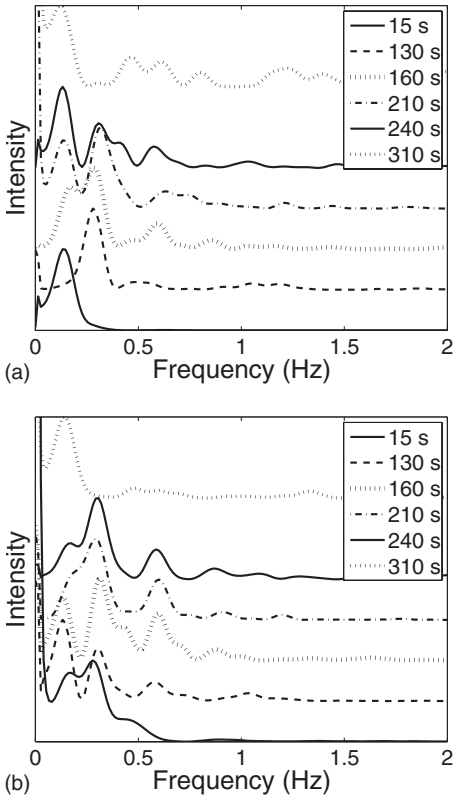

FIG. 12. Power spectra of x and y component velocities (u,v) at point 2.

same frequency as the plate frequency, whereas the v component has a frequency twice the plate frequency. Additionally these multiple frequencies were not observed in the case of viscoelastic fluids [19].

In this work it is interesting to note the appearance of multiple frequencies as higher harmonics at 130 s $(2f)$, due to the changing viscoelastic nature of the fluid. Unlike the regular viscoelastic fluid (where the changes in the property of fluid are not much significant), the reactive fluid property changes are gradual. These gradual changes in reactive fluids can be observed from the rheological measurements as shown in Figs. 4 and 3(b). The intensity of these higher harmonics increases with time as the reaction proceeds. At 240 s and higher, as there is no motion in the cavity, the reaction goes to completion and solidlike gel forms. Later the plate frequency dominates and the higher harmonics disappear. Thus the appearance and disappearance of these higher harmonics can give us information about the progress of the reaction. To analyze the presence of multiple frequencies in detail, the analysis was carried out at several points in the cavity.

The spectra at points 3 and 4 are shown in Fig. 13. At point 3, which is at the top corner of the cavity, the u component has a single dominant plate frequency in the spectra. The v-component spectra have multiple frequencies which are not higher harmonics. These multiple frequencies can be attributed to noise as the magnitude of the v-component velocity is very small when compared to the u component. At point 4, which is at the bottom of the cavity, both u- and v-component spectra show multiple frequencies which are

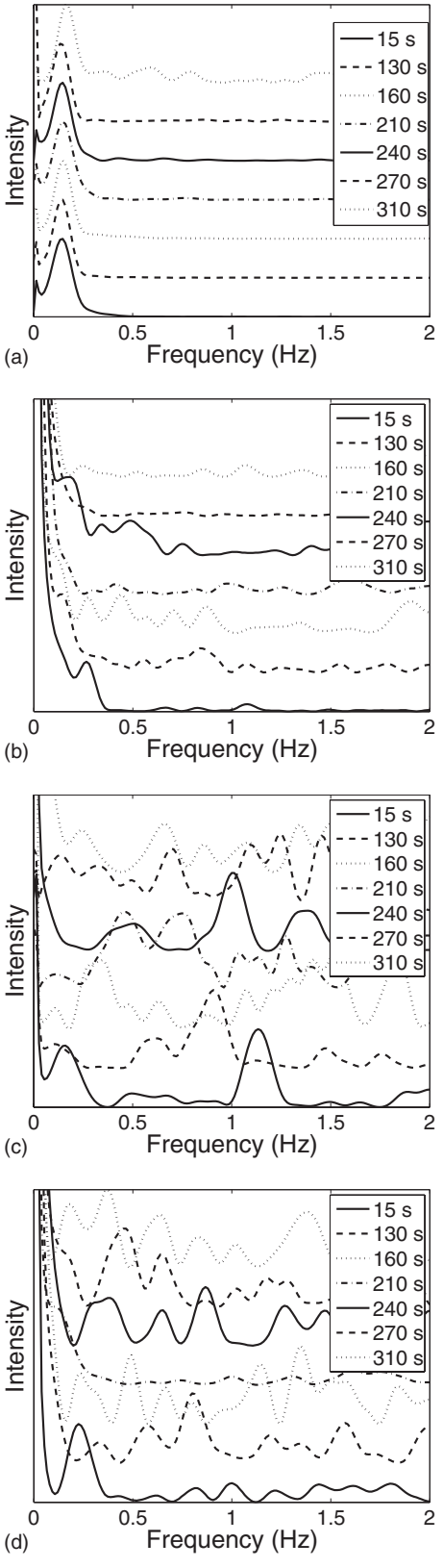

FIG. 13. Power spectra of x- and y-component velocities (u,v) at points 3 and 4.

not higher harmonics at all reaction times as shown in Fig. 13. As the magnitude of the u- and v-component velocities is very low at the bottom of the cavity, it is difficult to probe

the characteristics of the fluid. Hence these multiple frequencies are attributed to noise in the spectra. Also it was observed that as we go along the depth of the cavity, the higher harmonics disappear for the u component as the magnitude u will be reduced. For the v component they appear at the central plane and disappear near the walls as the magnitude of the v component is large in the central plane.

Multiple frequencies, which are higher harmonics, were also observed at other accelerator concentrations and plate speeds. In all these cases, the higher harmonics appear during gelation and disappear with time as the reaction goes for completion.

The influence of nonlinear elastic effects on the appearance of higher harmonics in oscillatory rheology has been analyzed earlier [20]. It should be noted that the higher harmonics in cavity flows were not observed for Newtonian fluids [12] and purely viscous shear thinning fluids [19]. To analyze the viscoelastic fluid flow in cavities, a primitive model such as the upper-convected Maxwell model can be used. However, it has also been shown that viscoelastic fluid flow (with polymer solutions) such higher harmonics was not observed [19]. During gelation, material transformations can be captured based on the viscosity change (purely viscous effect) or based on the change in relaxation times (viscoelastic effect) [21,22].

It would be very useful to solve the above problems for the case of cavity flows to investigate the origins and mechanisms of higher harmonics reported in the present work.

IV. SUMMARY

In the present work, we examined the gelation of PSA in a periodically driven cavity using PIV. The experiments were carried out at different plate velocities and by varying the amount of accelerator. The temporal and spatial variations of the velocity components were analyzed. The magnitude of the velocity components was found to decrease with progress of the reaction due to gel formation. The gel time observed from the velocity measurements was found to be in close agreement with those obtained from rheology. The role of mixing on the reaction was understood from the amount of gel formed at different plate velocities. Multiple frequencies which are higher harmonics in the velocity field were observed during the course of reaction. These higher harmonics were not observed when the reaction went to completion. Further theoretical investigations and simulations to examine the mechanisms of these higher harmonics would be of great interest.

ACKNOWLEDGMENTS

We would like to thank G. Santhosh Kumar, IIT Madras, for his help in the analysis of the experimental data.

[1] H. H. Winter and M. Mours, Adv. Polym. Sci. **134**, 165 (1997).
[2] W. B. Young, K. Rupel, K. Han, L. J. Lee, and M. J. Liou, Polym. Compos. **12**, 30 (1991).
[3] L. P. Yeo, Y. H. Yan, Y. C. Lam, and M. B. Chan-park, Langmuir **22**, 10196 (2006).
[4] H. Zhang, E. Tumarkin, R. Peerani, Z. Nie, R. M. A. Sullan, G. C. Walker, and E. Kumacheva, J. Am. Chem. Soc. **128**, 12205 (2006).
[5] Y. K. Cheung, B. M. Gillette, M. Zhong, S. Ramcharan, and S. K. Sia, Lab Chip **7**, 574 (2007).
[6] D. G. Thomas, R. Sureshkumar, and B. Khomami, Phys. Rev. Lett. **97**, 054501 (2006).
[7] C. K. Aidun, N. G. Triantafillopoulos, and J. D. Benson, Phys. Fluids A **3**, 2081 (1991).
[8] M. Nallasamy and K. K. Prasad, J. Fluid Mech. **79**, 391 (1977).
[9] A. K. Prasad and J. R. Koseff, Phys. Fluids A **1**, 208 (1989).
[10] R. Iwatsu, J. M. Hyun, and K. Kuwahara, J. Fluids Eng. **114**, 143 (1992).
[11] M. J. Vogel, A. H. Hirsa, and J. M. Lopez, J. Fluid Mech. **478**, 197 (2003).
[12] S. Sriram, A. P. Deshpande, and S. Pushpavanam, J. Fluids Eng. **128**, 413 (2006).
[13] N. Ramanan and G. M. Homsy, Phys. Fluids **6**, 2690 (1994).
[14] V. O'Brien, ASME Trans. J. Appl. Mech. **42**, 557 (1975).
[15] C. W. Leong and J. M. Ottino, Phys. Rev. Lett. **64**, 874 (1990).
[16] P. Pakdel, S. H. Spiegelberg, and G. H. McKinley, Phys. Fluids **9**, 3123 (1997).
[17] T. Yamamoto, M. Ishiyama, M. Nakajima, K. Nakamura, and N. Mori, J. Non-Newtonian Fluid Mech. **114**, 13 (2003).
[18] F. Chambon and H. H. Winter, J. Rheol. **31**, 683 (1987).
[19] S. Sriram, A. P. Deshpande, and S. Pushpavanam, Polym. Eng. Sci. **48**, 1693 (2008).
[20] M. Wilhelm, D. Maring, and H.-W. Spiess, Rheol. Acta **37**, 399 (1998).
[21] K. Venkateshan and G. P. Johari, J. Chem. Phys. **125**, 014907 (2006).
[22] M. Mours and H. H. Winter, Macromolecules **29**, 7221 (1996).